Remaining Life Assessment of Hydrogen Pipelines for Flaw Sizes Below ILI and NDE Detection Limits

Zahra Lotfian, Michiel Brongers
Kiefner and Associates, Inc.

Organized by

https://doi.org/10.52202/078572-0016

https://doi.org/10.52202/078572-0016

Abstract

While pressure cycle fatigue may not typically be a significant concern in conventional gas pipelines, introducing hydrogen changes the dynamic. Hydrogen embrittlement accelerates crack growth rates and reduces material toughness, making pressure cycle fatigue analysis a critical component of mechanical integrity assessments. As the industry shifts towards hydrogen blending in natural gas pipelines, accurate remaining life assessments become essential for effective integrity management, particularly for small flaw sizes undetectable by in-line inspection (ILI) or non-destructive evaluation (NDE) tools.

As part of ongoing research [1] for the United States Department of Transportation (USDOT) Pipeline and Hazardous Materials Safety Administration (PHMSA), this paper addresses the challenge of assessing flaws at or below detection thresholds. The remaining life of these flaws was estimated through a series of case studies, accounting for variables such as flaw size, fracture toughness, pipe geometry, and the severity of pressure cycles. Advanced fatigue models, capturing crack growth across Regions I (threshold), II (stable growth), and III (rapid growth), were employed, integrating experimental fatigue crack growth rate (FCGR) data to reduce conservatism compared to traditional upper-bound design curves.

Results indicate that hydrogen environments significantly accelerate fatigue compared to air. Most cases exhibited leak-before-break behavior. Notably, mild to moderately aggressive pressure cycles and small flaws demonstrated long fatigue lives exceeding 100 years in a gaseous hydrogen environment. Such flaws are relatively fatigue-insensitive and can be adequately evaluated using simpler models and hydrogen fatigue design curves. However, aggressive pressure cycles and larger flaws (exceeding 40% of wall thickness) markedly reduced pipeline life, particularly under reduced fracture toughness conditions. Furthermore, while lowering the fracture toughness from an average value of 90 (ksi$\sqrt{\text{in}}$) to the ASME B31.12 minimum of 50 (ksi$\sqrt{\text{in}}$) had a minor impact under mild pressure cycle conditions, further reductions dramatically decreased fatigue life, emphasizing the importance of material selection.

Introduction

The global shift towards hydrogen as a clean energy source has brought significant attention to pipeline mechanical integrity. Hydrogen's unique properties, such as its propensity to embrittle pipeline materials, accelerate FCGRs and reduce fracture toughness, posing challenges to safety and reliability that conventional analysis methods cannot adequately address. These issues are further compounded by the industry's move to blend hydrogen with natural gas, where undetected subcritical flaws may grow critical over time, threatening aging infrastructure.

https://doi.org/10.52202/078572-0016

This study aims to bridge this gap by providing operators with insights into the remaining life of flaws below the detection limits of ILI and NDE tools in hydrogen-exposed pipelines. It focuses on integrating advanced fatigue models and experimental data to evaluate fatigue behavior across different crack growth regions, moving beyond traditional approaches to ensure mechanical integrity in hydrogen environments.

Reinspection Intervals

Theoretically, a pipeline's life can be infinite if maintained adequately. However, pipeline integrity is threatened by various causes that must be managed to ensure safe operations. Codes such as ASME B31.8S-2018 [2] list specific integrity threats, usually associated with the pipe's physical features and metallurgical conditions. Integrity management programs (IMPs) rely on ILI to find those features.

Once the feature locations are located, their identity is positively established, their current dimensions are known, a likely future growth rate is known, their anticipated remaining life can be estimated, and appropriate responses can be executed. These activities must be done on a schedule, with reinspection/reassessment before the feature becomes critical. Thus, to avoid failure, the reinspection interval (RI) should be set shorter (for example, half) than the remaining life (RL).

Operators should evaluate all detected features and estimate their individual remaining lives. The feature with the shortest life will be “the weakest link” that dominates the life of the entire pipeline. The operator should repair or remove/cut out all features with a remaining life shorter than the desired reinspection interval (for example, five years).

In addition to the parameters mentioned above, the following is a non-exhaustive list of things that should be considered in the RL determination:

- Basic pipeline design, steel properties, and operational details - through data integration,
- Diameter, wall thickness (wt), specified minimum yield strength (SMYS) and ultimate tensile strength (UTS), assumptions on material properties,
- Seam weld type, vintage, coating type, cathodic protection (CP) or no CP,
- Maximum allowable operating pressure (MAOP), pressure fluctuations, temperature, known history, threat identification and interaction,
- Properties of sub-critical size features,
- Characteristics at time of inspection (probability of detection, identification, sizing),
- Estimated growth rates,
- Assumptions on growth mechanism,
- Assumptions on rate with time (constant or changing rate),
- Properties of critical size features,

https://doi.org/10.52202/078572-0016

- Definition of failure (depth-through-wall percentage, flow strength, fracture toughness),
- Uncertainty in all parameters,
- Decision on reinspection interval,
- If half of the RL is sufficient, and
- The length of the desired interval.

The process of establishing a reinspection interval is illustrated in Figure 1 through Figure 5. The period of interest is operations, which can last many decades. Periodic maintenance should be planned, and operators typically have a system to ensure these standard activities are accomplished. If maintenance is performed such that anomalies never reach critical dimensions, the pipeline's life can be infinite, as illustrated in Figure 1.

Features other than pipe manufacturing defects initiate sometime after the pipeline is placed into service. For example, it takes time before a coating disbands, and corrosion metal loss can occur on the metal surface. From the moment a feature initiates, it can grow at a rate determined by the growth mechanism and environmental and operational conditions. Failure is usually defined as the instant that a feature has grown to a critical size, causing the pipe to leak or rupture. Thus, the total feature life from initiation to a critical size is shown in Figure 2.

Features cannot be identified at the time of initiation because they are too small. Sometime later, during the feature's subcritical life, it can be detected by an inspection. The time between the moment that a feature is detected/identified and the time that it grows to critical size is the remaining life of the feature; refer to Figure 3.

The reinspection interval should be set well before a feature becomes critical. A typical value engineers use is a Factor 2, signifying the RI should not exceed half of the RL; refer to Figure 4. For a collection of features, such as the entire collection of anomalies detected in an ILI run, the shortest RL of a feature dominates and limits the pipeline's RL. The desired RI can be reached by repairing/removing those features with the shortest RL. The non-repaired features should be monitored until the next inspection/assessment; refer to Figure 5.

https://doi.org/10.52202/078572-0016

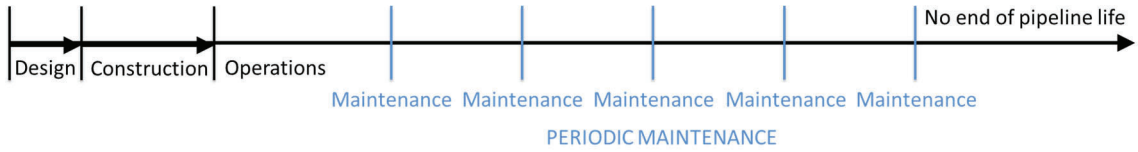

Figure 1. Timeline showing periodic maintenance at regular intervals during pipeline operation.

Figure 2. Timeline showing feature life from time of first initiation with feature growth until the feature's critical size is reached.

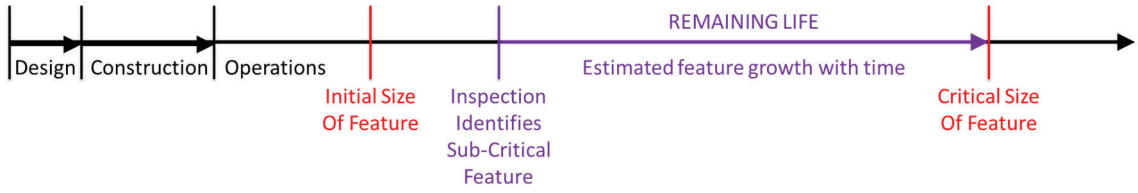

Figure 3. Timeline showing remaining life is shorter than the total feature life.

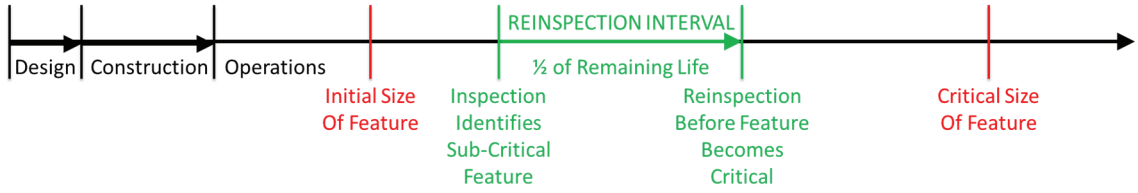

Figure 4. Timeline showing a reinspection interval of a single feature as half of the feature's remaining life.

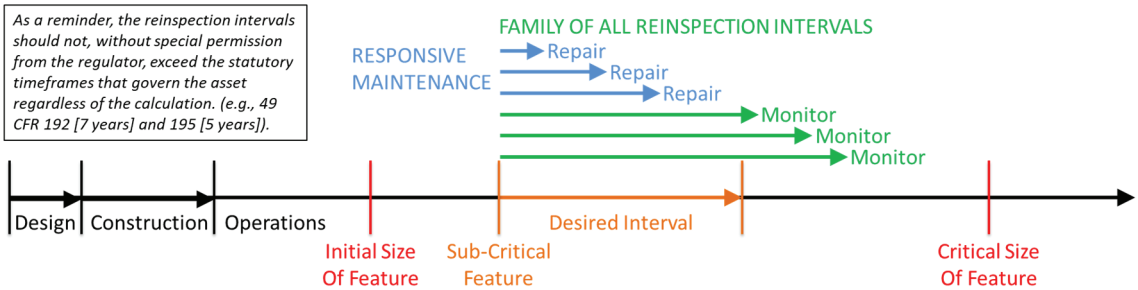

Figure 5. Timeline showing that the desired (reinspection) interval of a collection of features is determined by the shortest remaining life of any single feature that is not repaired.

https://doi.org/10.52202/078572-0016

Methodology

Fracture Mechanics Concepts

The steel's fatigue response is characterized by three regions, generally referred to as Region I (threshold), Region II (stable crack growth), and Region III (rapid crack growth); see Figure 6. Most pipeline fatigue analyses focus on Region II, represented by a power law relationship between the crack growth rate (da/dN). This is the change in crack depth, a, per cycle, N, and the stress intensity factor range, ΔK. This relationship is the Paris equation, where C and n are curve-fitting parameters. A limitation of the Paris equation is that the FCGR in Region I is modeled unrealistically fast and in Region III unrealistically slow.

$$\frac{da}{dN} = C\,(\Delta K)^n \qquad \text{Paris equation}$$

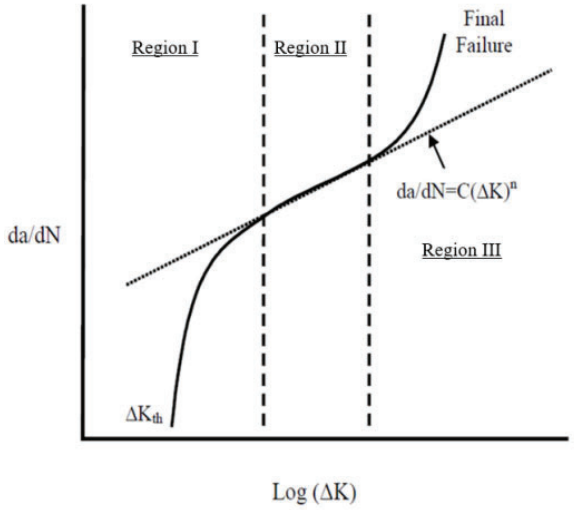

Figure 6. Fatigue crack growth rate in different regions

With the introduction of hydrogen into existing pipelines and the emerging need for pipeline crack growth management, this study considers a more advanced crack growth analysis. It represents the full spectrum of the behavior in low, medium, and high ΔK regions. The Walker equation modifies the Paris equation, providing a parameter (m) to adjust the magnitude of the data shifting as a function of the load ratio (R). This is important because laboratory test data are often limited to a few R-ratios. The Walker equation allows adjustment without requiring retesting at many different R-ratios,

$$\frac{da}{dN} = C\left(\Delta K(1-R)^{(m-1)}\right)^n \qquad \text{Walker equation}$$

in which da is the change in crack dimension, N is the incremental load cycle, K is the stress intensity factor, R is the minimum to maximum load ratio in the cycle, C and n are growth constants, and m is the stress shift parameter.

https://doi.org/10.52202/078572-0016

Experimental Test Data

In this study, experimental FCGR test data measured in laboratory-scale experiments with hydrogen environments are used to reduce conservatism in the analysis by replacing standard fatigue design curves, such as those in ASME B31.12 [3], with empirical data. This approach provides a more accurate representation of crack growth within the specific data range considered. This study used FCGR test data in hydrogen from Sandia National Laboratories (SNL), which was developed as part of the HyBlend project [4]. These data are also included in the AFMAT fracture mechanics database [5], which is integrated into the AFGROW fatigue crack growth analysis software tool used in this study. Originally developed by the Air Force Research Laboratory and now maintained by LexTech, Inc., AFGROW is widely used for fatigue analysis in the aerospace and nuclear industries. It incorporates the Harter T-method [6, 7] to determine crack growth rates for different R-ratios from just a few ΔK-da/dN curves.

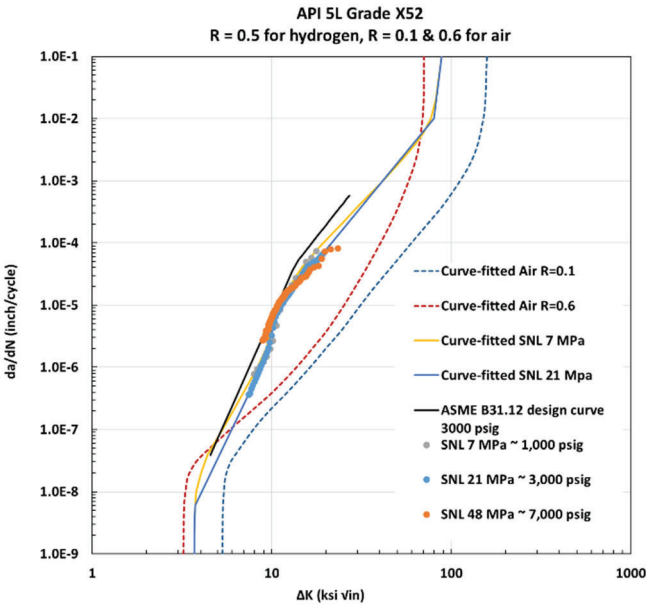

Figure 7. FCGR curves for API 5L Grade X52 line pipe steel samples tested in hydrogen and in air, based on data from SNL and ASME B31.12 design curve.

Figure 7 shows an example of the SNL data for an API 5L Grade X52 line pipe steel tested in the base metal in a 100% hydrogen environment at R = 0.5 under three different hydrogen pressures. The data at 7 MPa (1,000 psig) and 21 MPa (3,000 psig) are particularly relevant to the range of interest for pipelines repurposed for hydrogen service. Due to challenges in collecting experimental test data at the extreme lower and upper thresholds, the SNL data primarily covers Region II. This study's data have been curve-fitted based on the SNL 21 MPa[1] base metal data to extend coverage to

[1] The 21 MPa base metal data were selected for this study because the SNL database contains only fusion zone and heat-affected zone (HAZ) data at this pressure. This enables future studies to explore the effects of base metal versus HAZ and fusion zone.

https://doi.org/10.52202/078572-0016

these threshold regions. The value m in the Walker equation is determined using the Harter T method from these experimental test data.

The experimental test results show minimal variation and negligible differences when extended to line pipe steel Grades X42 and X60. Similar FCGR data for air at R = 0.1 and R = 0.6 are also plotted for comparison. When comparing the growth rates in hydrogen with those in air, it is evident that, for typical ΔK values, the air curves exhibit significantly lower FCGRs than the hydrogen curves. However, at the limiting edges, the hydrogen-charged data appear to converge to the air FCGR data in Regions I and III (for the same R-ratio).

Inputs to Fatigue Model

Case studies were performed considering various pipeline conditions, including flaw size, fracture toughness (also called fracture resistance), and pressure cycle severity. Hill et al. [8] and Schroeder et al. [9] conducted a sensitivity study of the effects of hydrogen on line pipe integrity.

Critical Flaw Size

In this study, cracks were modeled to propagate until they reached the critical crack size, beyond which further growth would become unstable. At that point, the pipe was considered to have failed. The critical crack size was defined as the flaw dimensions for which the applied stress intensity factor, $K_{applied}$, from the pressure-induced hoop stress equaled the material's fracture toughness, K_{mat}. When $K_{applied} \geq K_{mat}$, failure is predicted. This condition can occur in two scenarios:

- Before the critical crack depth, a, reaches 80%[2] of the wall thickness (a_{crit} < 80% of the wt). This scenario could occur for materials with low toughness or very long cracks in more ductile steels.
- After the crack depth becomes through-wall. This scenario is more favorable as it represents a leak-before-break condition, allowing for potential detection and mitigation before catastrophic failure.

Additionally, a failure assessment diagram (FAD)-based approach can be used to transition to a through-wall crack, employing methods described in API 579-1/ASME FFS-1-2021 [10], such as CorLAS™ [11]. A few cases were studied using such the FAD approach to critical flaw size.

The analysis begins with an initial crack size and progresses iteratively until the critical crack size is reached. The stress intensity factor range (ΔK) for each cycle increment is calculated for the flaw's length and depth directions based on its current size and the pipeline loading conditions. Using an FCGR curve, the crack advancement rates in the length and depth directions are determined from the corresponding ΔK values, considering the specific R-ratio for that cycle. The crack depth and

[2] 80% wt is the threshold typically used to assume a through-wall crack.

https://doi.org/10.52202/078572-0016

length are then updated individually. After each update, the critical condition is evaluated. If the critical crack size is reached, the crack growth loop terminates.

Size of Flaws

ASME B31.12 does not specify initial flaw sizes for fatigue analysis. These must be considered as known or assumed anomaly sizes arising from either manufacturing workmanship acceptance criteria, NDE inspection, or survivable anomalies from hydrotest. Table 1 provides examples of typical features and their detectable minimum sizes using different ILI techniques based on data provided by Novitech, Inc. [1212] for their Micron MFL and Deformation ILI tools.

Table 1. Summary of detectable feature sizes for the Micron ILI Novitech tools.

Feature Type	ILI Technique	Detectable Minimum Size	Probability of Detection
Metal Loss (General, Pitting, Axial Grooving, Circumferential Grooving)	Axial MFL	10% of wt	95%
Metal Loss (Pinholes, Axial Slotting, Circumferential Slotting)	Axial MFL	20% or 10% of wt[3]	95%
Crack-like (Narrow Axial)	Circumferential and Axial MFL	20% of wt	>90%
Crack-like (Narrow Circumferential)	Circumferential and Axial MFL	25% of wt	>90%
Deformations	Geometry Tool	The greater of 0.5% OD or 0.030 inches	>99%

Since the detectable flaw size ranges vary between vendors, can be dependent upon ILI run quality, and may even vary between different tools from the same vendor, the present study analyzed a range of practical depths and lengths for undetected features to ensure comprehensive coverage as shown in Table 2. Initial flaw depth (a_0) values are expressed as a percentage of the wall thickness. As will be discussed next, the effect of pipe grade on fracture toughness has already been accounted for, and therefore, the analysis focused solely on Grade X52 for the case studies.

[3] Minimum detectable size is dependent upon the width and length of the metal loss found; further details are located in the source documentation.

https://doi.org/10.52202/078572-0016

Table 2. Input parameter values used in sensitivity studies.

Property	Base Case Value	Range of Tested Values
Flaw Depth, a_0/wt	60%	5%, 10%, 15%, 20%, 40%, 60%, 80%
Flaw Length	3 in	0.5, 1.0, 1.5, 2.0, 3.0 in
Pipe OD/wt	10 /0.25 (in/in)	10/0.25, 20/0.50 (in/in)
Fracture Toughness (Plane Strain/Plane Stress)	90/176 (ksi√in)	90/176, 50/98, 40/78, 30/59, 25/49, 20/39 (ksi√in)
Maximum Operating Pressure (MOP) and Spectrum Severity Indicator (SSI)	50% SMYS, 25	50% SMYS/25, 72% SMYS/75

Fracture Toughness and Pipe Grade

Material strength (grade) and fracture toughness (fracture resistance) are correlated, and a general trend for steels is that susceptibility to hydrogen embrittlement increases with higher material strength. Studies [1213, 14, 15] show that the Mode I threshold stress intensity factor in hydrogen, K_{IH}, decreases as yield strength increases. Based on tests conducted by Ronevich et al. [16], the average fracture resistance under plane strain conditions was approximately 100 MPa√m (91 ksi√in) for line pipe Grades X42 and X52 and approximately 80 MPa√m (73 ksi√in) for Grade X60.

The maximum applied stress intensity factor, K_{IA}, can be calculated for given flaw dimensions at design pressure. For the flaw to survive, K_{IH} shall be equal to or higher than the calculated value of K_{IA}. In any case, ASME B31.12-2023 requires that the K_{IH} of a material shall not be less than 55 MPa√m (50 ksi√in).

Considering these findings, two ranges of plain strain fracture toughness were selected for the primary evaluation: a minimum of 50 ksi√in and an average of 90 ksi√in. Corresponding plane stress fracture toughness values were proportionally set at 98 ksi√in (minimum) and 176 ksi√in (average). Other lower fracture toughness values were also analyzed to observe the trend of fatigue life for extremely low-toughness situations.

Flaw Geometry and Location on Weld or Base Metal

This study assumed the same crack geometry prescribed in ASME B31.12: axially oriented semi-elliptical surface flaw on the inner pipe wall surface. The stress intensity factor solution and the reference stress solution for the given geometry were calculated using the API-579 solution manual.

Tests conducted by SNL [16, 17] showed that a weld's fusion metal and HAZs exhibit similar fatigue crack growth behavior in hydrogen environments as base metals, provided residual stress is accounted

https://doi.org/10.52202/078572-0016

for. Similar trends have also been observed across various welding processes. Consequently, this study does not account for the specific location of the flaw with respect to welds.

Pipe Geometry

Two outer diameters (ODs) of 10 and 20 inches were considered, paired with wt of 0.25 and 0.50 inches, respectively. Both cases maintain an OD/wt ratio of 40, a typical value for transmission pipeline applications.

Pressure Cycle Severity

To evaluate the effect of internal pressure cycles, two spectra with similar trends but varying levels of severity were applied in this study. The spectrum severity indicator (SSI) is a parameter that quantifies the severity of cyclic fatigue associated with the pressure time history. SSI is the number of cycles of characteristic stress that results in the same fatigue damage (i.e., crack growth) as the actual pressure time history annually. The standard SSI definition is based on the hoop stress range of 13 ksi, which was used in this study. For more information on SSI, refer to the 2018 paper by Semiga et al. [18].

The first pressure spectrum used in the study had an actual maximum operating pressure (MOP) of 1,300 psig, corresponding to 50% of the SMYS, and an SSI of 25, which is classified as mild cycling for a gas pipeline. The second pressure spectrum had an actual MOP of 1,872 psig, representing 72% of SMYS, with an SSI of 75, classified as moderate to aggressive cycling for a gas pipeline. The selection of these two spectra, based on their MOP, reflects the upper bound of the design pressure limits for Option A (prescriptive design) and Option B (performance-based design) as defined in ASME B31.12-2023. The analysis accounts for the characteristics of the pressure cycle, including the sequence of cycles and the amplitude of individual cycles.

Discussion of the Results

The reported fatigue life intentionally does not include safety factors and is presented as calculated. A base case was analyzed, serving as the benchmark for comparing other cases. Using the base case parameters, Figure 8 illustrates depth and length growth versus the number of cycles on a logarithmic scale, comparing behavior in a 100% hydrogen gas environment to that in air. The results show that the fatigue life in air is approximately one order of magnitude larger than in hydrogen. This trend remains consistent even when larger pipe diameters or more aggressive pressure cycles are considered.

Additionally, both air and hydrogen cases exhibit a leak-before-break scenario. The program assumes a through-wall crack when the flaw depth reaches 80% of wt. However, because the applied stress intensity factor, $K_{applied}$, for the through-wall crack, has not yet reached the fracture toughness of the material, K_{mat}, the through-wall crack will propagate in the axial (length) direction until K_{mat} is achieved.

https://doi.org/10.52202/078572-0016

In a separate analysis, the effect of wall thickness was evaluated for two pipes with the same OD/wt ratio. Figure 9 shows that, as expected, pipes with a lower wall thickness consistently exhibited shorter fatigue lives due to the reduced remaining ligament for flaws with the same length and depth-to-wt ratio. Additionally, the figure highlights how the more severe pressure cycles result in a decrease in fatigue life.

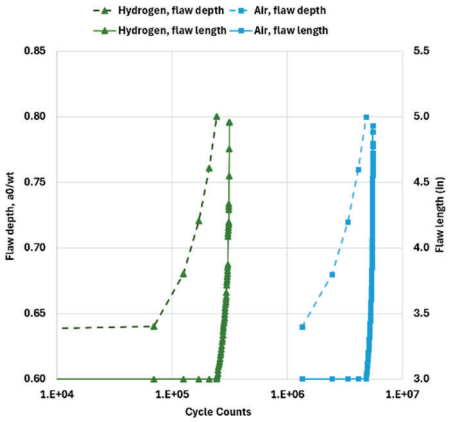

Figure 8. Normalized flaw depth and length growth vs. the number of cycles in hydrogen and air.

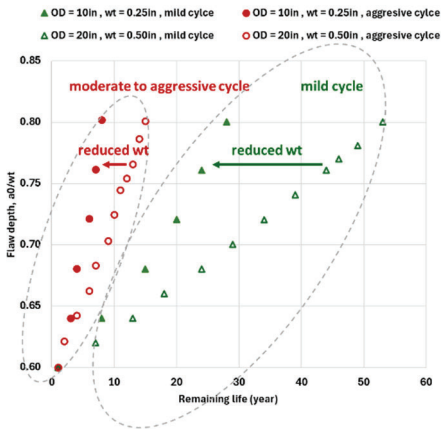

Figure 9. Normalized flaw depth vs. remaining life[4] for various pressure cycle severity and pipe geometry.

Influence of Flaw Size, Pressure Severity, and Pipe Geometry

The results of four different flaw depths (a_0) were reported: 20%, 40%, 60%, and 80% of the wt. For each depth, sensitivity analyses were conducted at five flaw lengths (inches): 0.5, 1.0, 1.5, 2.0, 3.0, as shown in Figure 10 to Figure 13. These plots illustrate the calculated remaining life in years versus the combination of flaw length and normalized flaw depth (a_0/wt). The remaining life values exceeding 100 years are grouped under the ">=100 years" category. Smaller depths and lengths were tested but resulted in significantly longer fatigue life and are not reported here, as the trend was clear.

Overall, experimental hydrogen test results for pipeline steel, together with a more accurate fatigue model, showed that undetected flaws with depths less than 40% of the wt and lengths up to 3 inches on a pipeline with mild pressure cycles exhibited very long fatigue life, indicating fatigue insensitivity. For more aggressive pressure cycles, undetected flaws with depths up to 40% of the wt and lengths up to 1.5 inches showed fatigue life exceeding 100 years.

Additionally, cases involving larger OD and wt (with the same OD/wt ratio) demonstrated a fatigue life of approximately twice as long or more for larger flaw sizes. For more aggressive pressure cycles, the impact of crack depth was significant: changing the depth by a factor of 2 resulted in at least a

[4] For illustration purposes, the life cycles are plotted only until the crack reaches 80% of wt. Beyond this point, the crack is assumed to become through-wall and continue to grow in the longitudinal direction.

https://doi.org/10.52202/078572-0016

two-fold change in feature life. The effect of pressure cycle severity was particularly pronounced in smaller OD/wt pipes, especially for flaws with depths greater than 40% of the wt.

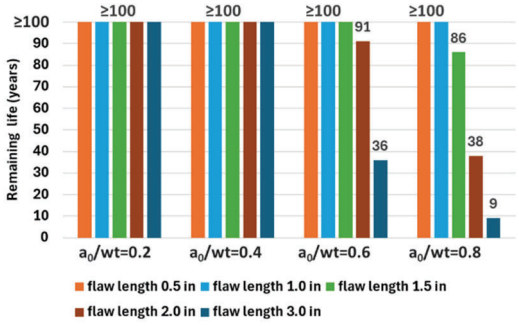

Figure 10. Remaining life for mild cycles, OD = 10 in, wt = 0.25 in.

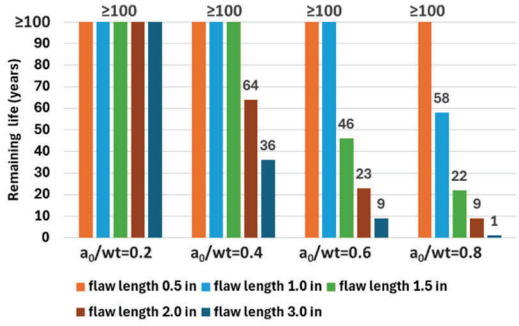

Figure 11. Remaining life for aggressive cycles, OD = 10 in, wt = 0.25 in.

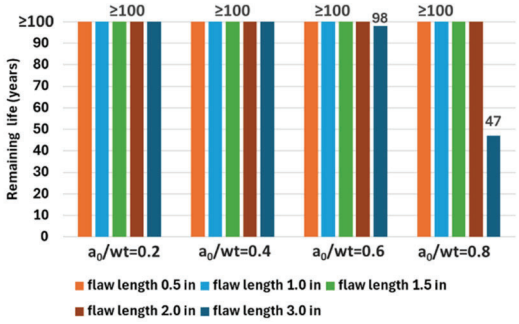

Figure 12. Remaining life for mild cycles, OD = 20 in, wt = 0.50 in.

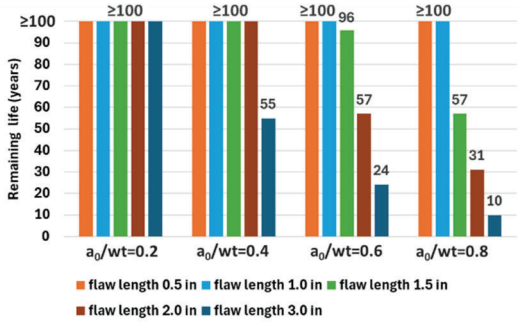

Figure 13. Remaining life for aggressive cycles, OD = 20 in, wt = 0.50 in.

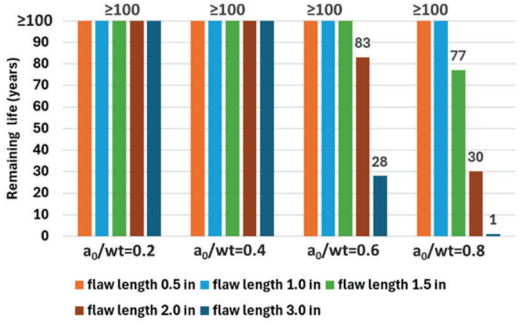

Figure 14. Remaining life for low toughness material, mild cycles, OD = 10 in, wt = 0.25 in.

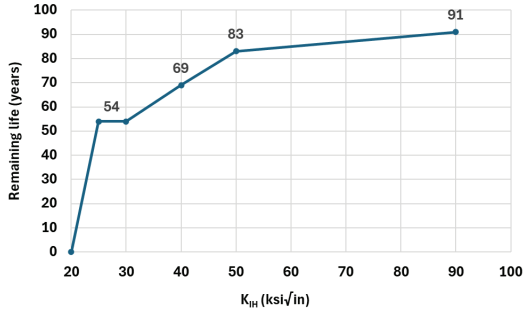

Figure 15. Remaining life based on K_{IH} fracture toughness, mild cycles, OD=10 in, wt = 0.25 in, a_0/wt = 0.6, flaw length = 2.0 in.

https://doi.org/10.52202/078572-0016

Influence of Fracture Toughness

Comparing the results in Figure 10 to those in Figure 14, it is evident that reducing the plane strain fracture toughness, K_{IH}, from the base case value of 90 ksi√in (and the corresponding plane stress toughness) to the minimum code requirement of 50 ksi√in results in only a slight reduction in fatigue life for flaws with depths exceeding 60% of the wt and lengths greater than 2 inches. However, further reductions in K_{IH} (and the corresponding plane stress toughness) lead to a more significant decrease in fatigue life, as illustrated in Figure 15. Notably, when K_{IH} drops below 20 ksi√in, the feature fails immediately, with no fatigue life remaining.

Influence of Criteria for End of Fatigue Life

Changing the transition criteria for defining through-wall cracks from 80% of the wt to the CorLAS™ model showed no significant impact on the remaining life for the base case values in Table 2 across the different flaw sizes tested. When fracture toughness was reduced to 50 ksi√in, the fatigue life for one case showed a slight reduction, but the effect was negligible. Overall, the 80% cut-off and the CorLAS model yielded similar results under typical conditions. The 80% cut-off is widely accepted as a threshold to avoid errors in stress intensity factor calculations when the remaining ligament becomes very small and plain strain conditions are no longer satisfied.

Most of the fatigue life reported in this study corresponds to cases where the crack transitions from a surface crack to a through-wall crack but continues to grow until it reaches the unstable growth condition ($K \geq K_{mat}$), marking the end of life. If, instead, the fatigue life is defined as ending when the crack becomes a through-wall (indicating leakage), the calculated fatigue life would be shorter. For the flaw sizes examined using the base case parameters, this difference in definition resulted in less than a 50% variation in fatigue life.

Recommendations and Future Research

Several parameters were not explored in this study, and further investigation is recommended:

- Material and Pipeline Conditions: Future research should examine fatigue life across a wider range of materials and pipeline conditions. For example, the pressure cycle spectrum used in this study ranged from mild to moderately aggressive. Assessing the effect of highly aggressive pressure cycling on hydrogen gas pipelines would be valuable. Additionally, incorporating probabilistic analyses to account for uncertainties would enhance understanding. Tools like the publicly available HELPR software [19], developed as part of the SNL HyBlend project, can facilitate such analyses using ASME B31.12 hydrogen FCGR design curves. Expanding these platforms to support actual FCGR test data would provide a significant advantage.
- Localized Effects on Welds: The impact of hard spots on welds, which can increase susceptibility to hydrogen-assisted fatigue, warrants further investigation. Similarly, the effect

https://doi.org/10.52202/078572-0016

of residual stresses, which can shift the effective ΔK in FCGR relationships, as reported in [20], needs further investigation.

- Hydrogen Concentration: This study focused on 100% hydrogen gas conditions. However, lower hydrogen concentrations (e.g., 1% or 10%) have been shown to moderately reduce fracture toughness and fatigue crack growth rates in the intermediate range of ΔK [**Error! Reference source not found.**].

Summary and Conclusions

As part of ongoing research for PHMSA, this study focused on assessing the remaining life of hydrogen pipelines with flaws of varying sizes, particularly those below the detection limits of ILI and NDE tools. An advanced fatigue model with the Harter T-method was used to analyze full-spectrum crack growth across Regions I (threshold), II (stable growth), and III (rapid growth). By incorporating experimental test data of actual FCGRs instead of conservative fatigue design curves, the study reduced conservatism and provided a realistic assessment of pipeline life. Key factors analyzed include flaw size, fracture toughness, pipe geometry, and pressure cycle severity, as summarized in Table 2.

The results indicated that fatigue life in air is approximately one order of magnitude greater than in 100% hydrogen gas across different pipe geometries and pressure cycle severities. Most analyzed cases exhibited a leak-before-break characteristic, where flaw depths reach 80% of the wt and are assumed through-wall before the applied stress intensity factor equals or exceeds the material's fracture toughness ($K_{applied} \geq K_{mat}$).

For mild pressure cycles, flaws with depths less than 40% of the wt and lengths up to 3 inches were shown to be fatigue-insensitive, with lifetimes exceeding 100 years. Under moderate to aggressive cycles, flaws up to 1.5 inches long and 40% of the wt still showed fatigue lives exceeding 100 years. The results further demonstrated that flaw depth significantly impacted fatigue life, with a doubling of depth leading to at least a two-fold reduction in life. Additionally, pipes with larger ODs and wt's but the same OD/wt ratio exhibited fatigue lives approximately twice as long or greater, particularly for larger flaw sizes or those under aggressive pressure cycles.

Reducing fracture toughness from the base case of 90 ksi√in (representing the average measured toughness) to the ASME B31.12 minimum requirement of 50 ksi√in has a minor impact on fatigue life. However, further reductions in toughness lead to a more significant decrease in fatigue life.

Experimental hydrogen fatigue test data reduces conservatism and provides a more realistic estimate of pipeline life in hydrogen environments than when conservative design curves are used. Simultaneously, advanced fatigue crack growth rate models that account for all three regions enhanced the accuracy of remaining life assessments. Long fatigue lives were predicted for mild pressure cycles and small flaw sizes typical for flaws undetected by ILI and NDE. Accordingly, more straightforward, conservative methods using design fatigue curves may be sufficient for their

https://doi.org/10.52202/078572-0016

assessment. However, aggressive pressure cycles combined with lower fracture toughness significantly amplified fatigue risks, highlighting the importance of considering a more thorough evaluation.

References

1. Investigate Damage Mechanisms for Hydrogen and Hydrogen/Natural Gas Blends to Determine Inspection Intervals for ILI Tools, Contractor: Kiefner and Associates, Inc., for U.S.DOT/PHMSA Project 693JK32310011POTA.
2. ASME B31.8S-2018, Managing System Integrity of Gas Pipelines, ASME Code for Pressure Piping, B31, Supplement to ASME B31.8, American Society of Mechanical Engineers (ASME), New York, NY, 2018.
3. ASME B31.12-2023, Code for Hydrogen Piping and Pipelines, ASME Code for Pressure Piping, B31, American Society of Mechanical Engineers (ASME), New York, NY, 2023.
4. Sandia hydrogen effect database https://granta-mi.sandia.gov/mi/index.aspx/; HyBlend - Technical Summary, U.S. Department of Energy (DOE) Office of Energy Efficiency and Renewable Energy (EERE), https://www.energy.gov/sites/default/files/2022-12/hyblend-tech-summary-120722.pdf, December, 2022.
5. AFMAT Fracture Mechanics Database, for AFGROW Version 5.3 Fracture Mechanics and Fatigue Crack Growth Analysis Software, https://www.afgrow.net/afmat.aspx
6. A History and Explanation of the Harter T-Method: Modeling Crack Growth Rate Data in a Tabular Lookup Format, J.A. Harter, LexTech, Inc., White Paper.
7. PRCI-REX2023-03 paper, Pipeline Steel Tubular da/dN Curves with Validations, Hydrogen Application, J. Harter, L. Lamborn, Contractors: LexTech, Enbridge Liquid Pipelines, for Pipeline Research Council International (PRCI), Houston, TX, 2023 Research Exchange, Paper, 7 March, 2023.
8. IPC2024-134020, Sensitivity Studies on the Evaluations of Hydrogen Effects on Linepipe Integrity Challenges, L. Hill, K. Bagnoli, E. Twombly, E. Punch, X. Gao, G. Wilkowski, Calgary, Alberta, Canada, ASME 2024 International Pipeline Conference (IPC), 23-27 September, 2024.
9. PVP2024-125226, Utilizing Probabilistic Analyses to Explore Performance Margins of Natural Gas Infrastructure for the Transport and Delivery of Hydrogen and Hydrogen Blends, B. Schroeder, C. San Marchi, J. Ronevich, M. Devin, J. Duell, & S. Potts., ASME 2024 Pressure Vessels & Piping Conference (PVP), July 29 - August 1, 2024.
10. API 579-1/ASME FFS-1-2021, Fitness-For-Service, 2021 Edition, American Petroleum Institute (API) / American Society of Mechanical Engineers (ASME), December, 2021.
11. CorLAS™, Crack Failure Pressure Calculator, DNV.
12. Micron ILI Tools: Probability of Detection (POD) and Sizing Tolerances for Features and Flaws, Novitech, Inc., Rev_2024-08-22.
13. Assessing Gaseous Hydrogen Assisted Fatigue Crack Growth Susceptibility of Pipeline Steel Weld Fusion Zones and Heat Affected Zones, J.A. Ronevich, B.P. Somerday, Sandia National

https://doi.org/10.52202/078572-0016

Laboratories (SNL), Materials Performance and Characterization, Vol. 5, No. 3, pp. 290-304, 6 September, 2016.

14. IPC2012-90313, Continued Microstructure and Mechanical Property Performance Evaluation of Commercial Grade API Pipeline Steels in High Pressure Gaseous Hydrogen, D. Stalheim, T. Boggess, D. Bromley, S. Jansto, S. Ningileri, American Society of Mechanical Engineers (ASME), Calgary, Alberta, Canada, ASME 2012 International Pipeline Conference (IPC), 24-28 September, 2012.
15. A Quantitative Description on Fracture Toughness of Steels in Hydrogen Gas, Y. Wang, J. Gong, W. Jiang, International Journal of Hydrogen Energy, Vol. 38, Issue 28, pp. 12503-12508, 19 September, 2013.
16. SAND2020-14066J, Hydrogen-Assisted Fracture Resistance of Pipeline Welds in Gaseous Hydrogen, J.A. Ronevich, E.J. Song, B.P. Somerday, C.W. San Marchi, Sandia National Laboratories (SNL), Somerday Consulting LLC, 2020.
17. Hydrogen Accelerated Fatigue Crack Growth of Friction Stir Welded X52 Steel Pipe, J.A. Ronevich, B.P. Somerday, Z. Feng, Sandia National Laboratories (SNL), Southwest Research Institute (SwRI), Oak Ridge National Laboratory (ORNL), International Journal of Hydrogen Energy, Vol. 42, Issue 7, pp. 4259-4268, 16 February 2017.
18. IPC2018-78717, Liquid Pipeline Location Specific Cyclic Pressure Determination, V. Semiga, A. Dinovitzer, S. Tiku, G. Vignal, American Society of Mechanical Engineers (ASME), Calgary, Alberta, Canada, ASME 2018 International Pipeline Conference (IPC), 24-28 September, 2018.
19. An Overview of the Hydrogen Extremely Low Probability of Rupture (HELPR) Toolkit for Probabilistic Structural Integrity Assessments when Transporting Hydrogen in Natural Gas Infrastructure, B. Schroeder, Sandia National Laboratories (SNL), Bellevue, WA, ASME 2024 Pressure Vessels and Piping Conference, EPRI Expert Workshop on Large-Scale Gaseous Hydrogen Infrastructure, Presentation 5D, 31 July - 1 August, 2024.
20. DIN CEN/TR 17797 09/2022, Gas infrastructure - Consequences of Hydrogen in the Gas Infrastructure and Identification of Related Standardisation Need in the Scope of CEN/TC 234, Deutscher Verein des Gas- und Wasserfaches e.V. (DVGW), Bonn, Germany, September, 2022.
21. PVP2018-84658, Influence of Hydrogen and Oxygen Impurity Content in a Natural Gas/Hydrogen Blend on the Toughness of an API X70 Steel, L. Briottet, H. Ez-Zaki, American Society of Mechanical Engineers (ASME), Prague, Czech Republic, ASME 2018 Pressure Vessels and Piping Conference, 15-20 July, 2018.

https://doi.org/10.52202/078572-0016